

A Compact Energy Harvesting RFID Tag for Smart Traffic Law Enforcement Systems

Shyama Wickramasinghe^{1, *}, Jeevani Jayasinghe², Gulam Nabi Alsath Mohammed³,
Melaka Senadeera⁴, and Malathi Kanagasabai⁵

Abstract—Currently, the inspection and verification of vehicle-related information are done by police inspectors using camera-based systems or manually. Though integrating video technology is more advantageous than manual operation, they do not perform accurately due to bad weather or driving styles. This paper presents the design of a compact, durable, battery-free, UHF RFID tag with enough memory to carry necessary information for automatic identification of traffic law enforcement applications. The vehicle owner can also be alerted when the tag is detected due to the visual indication facility. This tag’s novel feature includes adapting a modified T-match structure to match the highly capacitive impedance of the chosen RFID sensor chip, i.e., Farsens Rocky100. In contrast to existing designs, the proposed tag contains no extra lumped components that necessitate an external impedance matching circuit. Instead, the input impedance was matched using an advanced T-match topology and by optimizing the antenna’s geometrical features. Simulations were done in Ansys HFSS (High-Frequency Structure Simulator) whereas the dimensions of all the printed elements were fine-tuned using parametric optimization. The tag was fabricated on a low-cost FR4 substrate and measured. The tag with an overall size of $110 \times 25 \times 2.4 \text{ mm}^3$ can be detected by a conventional UHF RFID reader within a range of about 0.2 m–1 m. Due to the loop configuration, the tag exhibits a confined detection range while operating well within short ranges.

1. INTRODUCTION

The radio frequency identification (RFID) technology is expanding rapidly as a reliable, fast, and efficient approach for tracking and identifying objects using wireless communication [1]. An RFID system consists of tags that are attached to the objects to be identified and a reader to read the tags. The RFID tags come in battery-assisted (active) or battery-free (energy harvesting) forms [1]. In an energy harvesting RFID tag, its chip gets activated by the energy harvested from the antenna. Due to the unavailability of a battery, the energy harvesting tags are cheaper, smaller, lighter, and more durable. However, the optimal power transfer from the antenna to the chip happens only when their impedances match [2]. The impedance matching between the chip and the antenna can be achieved either using an external matching network or employing different internal impedance matching methods. The incorporation of external matching circuits is disadvantageous as they make the tag bulky, increase the cost of the tag, and make the manufacturing process more complicated. In contrast, internal impedance matching needs a more comprehensive scientific approach, particularly when the chip impedance is high.

Energy harvesting RFID tags work in several frequency bands, and those that operate in the UHF band (860 MHz–960 MHz) offer a longer read range and higher data transfer rate than other systems.

Received 18 May 2023, Accepted 10 July 2023, Scheduled 4 August 2023

* Corresponding author: Shyama Wickramasinghe (shyama@wyb.ac.lk).

¹ Department of Electrotechnology, Wayamba University of Sri Lanka, Kuliyaipitiya, Sri Lanka. ² Department of Electronics, Wayamba University of Sri Lanka, Kuliyaipitiya, Sri Lanka. ³ Department of Electronics and Communication Engineering, SSN College of Engineering, Chennai, India. ⁴ School of Arts and Sciences, Carolina University, North Carolina, USA. ⁵ Department of Electronics and Communication Engineering, College of Engineering Guindy, Anna University, Chennai, India.

Hence, they have been adopted in a wide range of fields such as supply chain management, logistics, asset tracking, and access control.

Over several decades, RFID technology has been employed in numerous automotive applications, primarily for identification [3] and tracking [4] of vehicles or parts at many stages during their life cycle including manufacturing, assembly, sales, tollgate collection [5, 6], etc. The use of RFID in the vehicle industry has expanded gradually, facilitating vehicle-to-vehicle communication [7], real-time traffic monitoring [8], traffic congestion control [9], smart traffic fine systems [10], prioritizing emergency vehicles through traffic control [11], etc. However, in most of these applications, active tags were used to enable long-range communication.

Due to the proven advantages of RFID technology, research studies are being expanded to check the possibility of adopting it to ease traffic law enforcement [12, 13]. Though camera-based traffic law enforcement systems are being broadly used, their efficiency depends on weather conditions, and the percentage of identified vehicles can drop to 40% as a result of rain, snow, and the road being dirty [12]. Further, they require battery power to operate. Driving styles such as frequently changing driving lanes and instant slowdowns near the cameras can also prevent the accurate identification in video-based systems [14].

In this context, energy harvesting UHF RFID tags have been identified as a potential candidate to address the research gaps in vehicle-related wireless communication applications as they are battery-free and have enough memory to carry vehicle information such as license plate number, vehicle model, and color [14].

However, the cost per tag is a key concern whereas over 50% of the total cost of the tag is spent on fabricating electronic components [15]. Internal impedance matching is useful in this context as external electronic components are not required in between the antenna and the chip. Among the limited number of related research works reported so far, an energy harvesting UHF tag with the size of $107 \times 29 \times 0.203 \text{ mm}^3$ designed incorporating a modified dipole antenna structure to facilitate toll collection by attaching it on the car windshield is presented in [6]. Another energy harvesting UHF RFID tag was designed employing a loop shape dipole antenna to be attached on automotive license plates or bumpers to recognize legally registered vehicles [16].

Aforementioned designs and a few other commercial products that are being used to track the vehicles optimized the antenna geometry to match the chip impedance by eliminating external matching components. However, those tags do not support sensor integration as the chips employed in them are conventional chips such as Impinj Monza [17] or Alien higgs [18]. As the conventional chips have low impedance, the chip's impedance could be simply matched by modifying the printed antenna employing a matching network that associates T-match [2, 19], nested slots [20], or inductively coupled loops [21]. In contrast, the Rocky100 chip [22] used in this design permits the integration of sensors, allowing additional, advanced functionality to be added to the tag.

Another major concern is the tag size. In order to achieve smaller tag sizes, recent research has focused on developing miniaturized energy harvesting RFID tags using numerous strategies such as meandering [23], fractals [24], and inverted F-structures [25]. Miniaturization is useful to reduce the cost of the tag as well [15]. Nevertheless, there was less effort made to miniaturize the energy harvesting RFID tags that facilitate sensor integration, thus they are bulky.

When RFID technology is used to streamline traffic law enforcement, it is important to identify a suitable detection range. As UHF RFID systems are usually long-range systems that work based on far-field backscatter coupling, their operational region is not confined [26]. As a result, they may detect all the tags that are available within the read range [26]. Thus, it is difficult for the police inspectors to confirm that the information the reader receives is of the vehicle to be checked. Further, the privacy of the vehicle owners is threatened as a reader kept several meters away from a far-field tag can retrieve and share the stored information anonymously [27]. In contrast, short-range RFID tags benefit due to confined read areas and avoid connecting with undesirable neighboring systems [26].

However, most of the energy harvesting UHF RFID tags do not support short-range communication [28]. Though there are many research publications on designing near-field UHF readers [1, 29, 30], only a few near-field UHF tags were reported [28]. Small broadband UHF tags designed in combination with T-match for impedance matching, meander lines for miniaturization, and loop feeding to enable short-range communication are presented in [28, 31]. The loop structure

allows the generation of a considerably large current, which results in a strong magnetic field enabling near-field applications [28]. However, integrating sensors to the above mentioned tags is impossible as conventional chips were used. Sensor-integratable chips solve the issue, but their impedance is highly capacitive, whereas matching it with no external electronic components is a challenging research task.

Addressing the demanding need of introducing a wireless RFID system with a tag that is battery-less, small, and sensor-integratable, this paper proposes the design of an energy harvesting UHF RFID tag for overcoming the issues related to traditional traffic law enforcement practices. The design of the RFID tag was started by employing a simple printed dipole antenna and a Farsens Rocky100 chip on a dielectric substrate. The very high chip impedance was matched by incorporating an advanced T-match topology into the antenna. Dipole arms were folded for antenna miniaturization. Simulations were carried out in Ansys HFSS (High-Frequency Structure Simulator) and the dimensions of all the printed elements were designed using parametric optimization. In order to validate the performance of the proposed tag, it was fabricated and measured.

The rest of the paper is structured as follows. The tag design methodology including internal impedance matching and miniaturization is explained in Section 2. Section 3 presents the simulated and measured tag performances in terms of the impedance, antenna bandwidth, and field patterns. Finally, the research findings are discussed, and the conclusions are given in Section 4.

2. DESIGN OF THE ENERGY HARVESTING TAG

2.1. Tag Configuration

Among the dual-mode UHF RFID chips reported in the literature, Farsens Rocky100 was selected after considering the sensitivity of the chip and the market availability. Its impedance is $64 - j469 \Omega$ at 868 MHz [22]. It has been used for developing battery-free RFID sensor devices since early 2019. Among RFID sensor chips, it has the highest capacitance in the input reactance (469Ω), thus implementing an internal impedance matching strategy is a challenge. Nevertheless, if the impedance matching of Farsens Rocky100 is possible, the same research methodology can be applied to any other RFID sensor chips as their capacitance is not that much high. Accordingly, the major objective of this research was matching the impedance of an energy harvesting UHF RFID tag antenna with that of the Farsens Rocky100 sensor chip without employing electronic components. The design of an RFID tag was started from employing a simple printed dipole antenna that has dimensions theoretically calculated to resonate around 868 MHz. Simulations were carried out in Ansys HFSS (High-Frequency Structure Simulator).

2.2. Internal Impedance Matching and Miniaturization

As reported in the literature, T-match configuration which is a combination of series and shunt inductors that boost the inductance was identified as a suitable impedance matching technique for the design of UHF RFID tags [32]. Hence, the design was modified incorporating a single T-match structure into the antenna, and parametric optimization was performed to identify the dimensions suitable for impedance matching. According to the simulation results, the single T-match structure improves tag performance in terms of the antenna impedance, but it could not achieve the highly inductive impedance required to match with the chip. The basic T-match structure was then modified by introducing a parallel bridge with length l_2 placed at a distance l_3 from the main dipole (Figure 1). Due to its loop configuration of the proposed novel structure, coupled with main dipole, the inductance of the antenna improves. Its geometrical parameters were optimized using parametric optimization to match the impedance. The length of the shorter dipole l_2 had a significant impact on the resonance frequency and antenna impedance. As a result of introducing a modified T-match topology with suitable dimensions, the antenna impedance was boosted to meet the chip's conjugate impedance. The overall size of the resultant dual-mode energy harvesting UHF RFID tag was $130 \times 25 \times 2.4 \text{ mm}^3$.

In order to reduce the tag length by applying miniaturization techniques, its dipole arms were folded thereafter (Figure 1). The geometrical parameters of the antenna and the matching network were tuned again using parametric optimization to reach the desired input impedance, i.e., $64 + j469 \Omega$ at 868 MHz, as detailed in our previously published paper [33]. The lengths of l_1 , l_2 , and l_3 had a major impact on the antenna's input impedance, and the optimized dimensions were $l_1 = 96.2 \text{ mm}$,

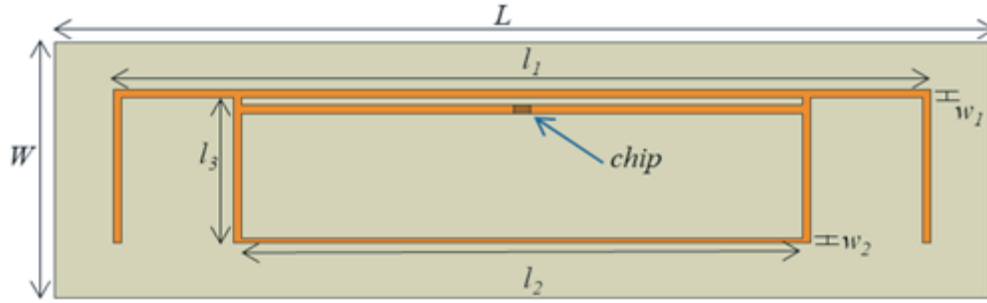


Figure 1. Proposed tag with the matching network.

$l_2 = 33$ mm, $l_3 = 17$ mm, $w_1 = 1$ mm, and $w_2 = 0.5$ mm. The overall tag size was finally reduced to $110 \times 25 \times 2.4$ mm³.

2.3. Fabrication

As illustrated in Figure 2, the energy harvesting tag was constructed in a low-cost FR4 substrate with relative permittivity of 4.4, thickness of 1.6 mm, and loss tangent of 0.002. As no lumped components were used for impedance matching, the chip was connected directly to the feed point of the antenna. A low-power (78 mW) LED that illuminates when the tag is detected by a UHF RFID reader was attached to the chip as a visual indicator.

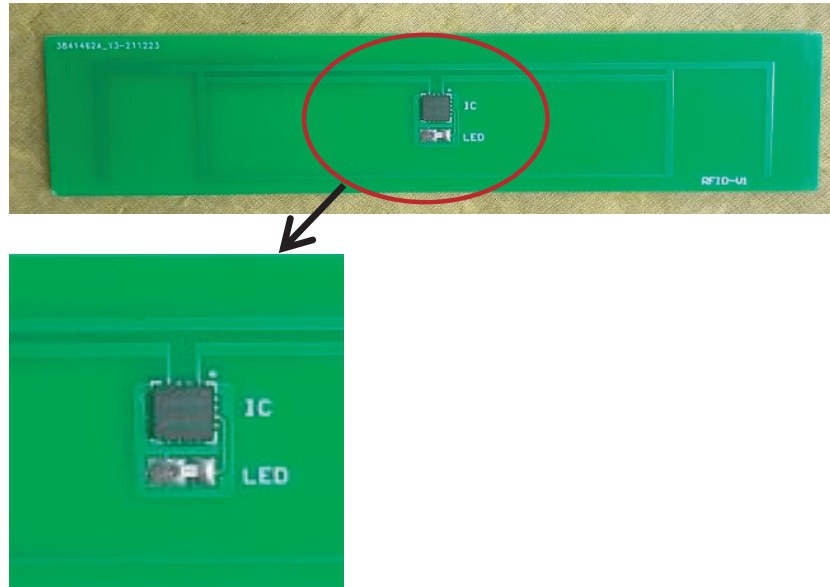


Figure 2. Photograph of the fabricated tag with the chip and a low power LED.

3. RESULTS AND DISCUSSION

3.1. Impedance

In order to guarantee the optimal performance of the tag, it is essential to accurately measure the antenna's input impedance. Figure 3 illustrates the simulated input impedance of the proposed antenna. According to the results, the antenna's input impedance at 868 MHz is $62.53 + j471.60 \Omega$. Hence, it matches well with the conjugate of the chip's impedance at the frequency of 868 MHz.

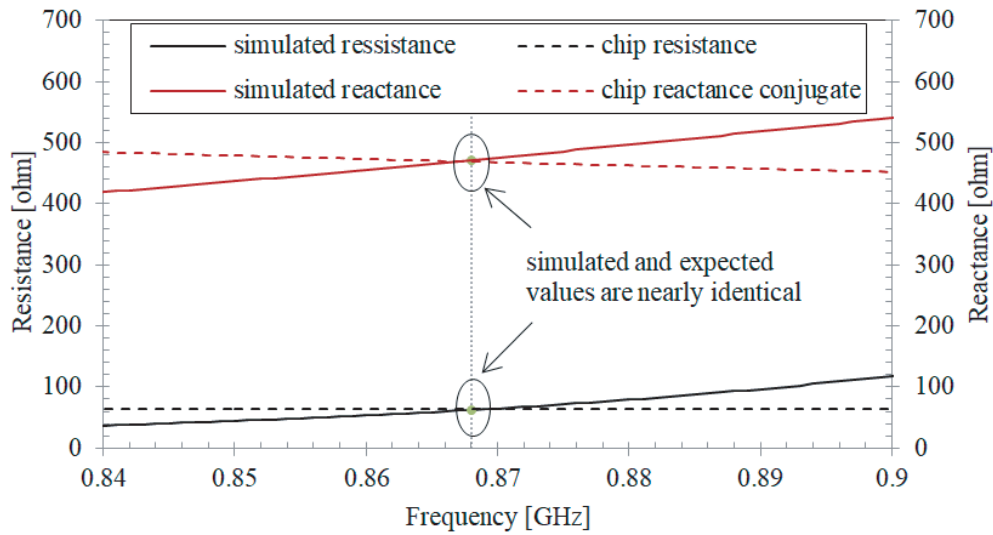


Figure 3. Simulated input impedance of the antenna.

Further, measurements were taken to validate the simulation results. As the proposed antenna is balanced and symmetrical, the Image Theory technique was used to measure its impedance using the setup shown in Figure 4. Half of the antenna was perpendicularly mounted on a 300 mm × 300 mm copper plate. The feed point of the antenna was soldered to the center pin of an SMA connector, and the other antenna arms were soldered to the copper plate. The SMA connector was attached to a Vector Network Analyzer (NanoVNA-F V2) to take S_{11} measurements.

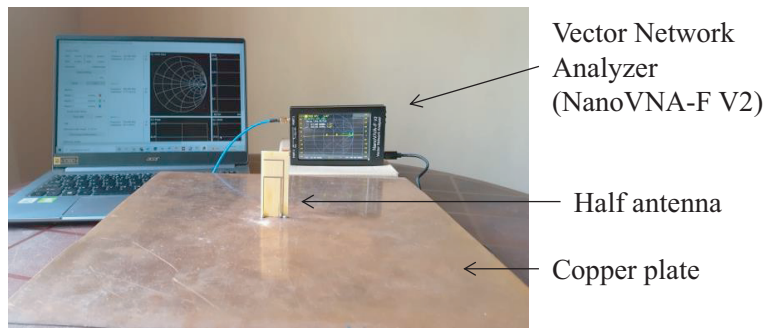


Figure 4. Impedance measurement set up using image.

Equation (1) was used to determine how the input impedance of the half antenna ($Z_{a, half}$) varies with frequency [34].

$$Z_{a, half} = \left(\frac{1 + S_{11}}{1 - S_{11}} \right) Z_0 \tag{1}$$

where S_{11} is the measured reflection coefficient, and Z_o represents the source impedance, which is 50 Ω. According to the image theory, the impedance of the full antenna is twice that of the half antenna. The calculated real and imaginary parts of the impedance are shown in Figure 5, together with the expected values. The results indicate that the impedance measured at 868 MHz, i.e., 68.96 + j444.93 Ω is reasonably close to the expected value.

Moreover, the power transmission coefficient τ ($0 \leq \tau \leq 1$) of the antenna was calculated by (2).

$$\tau = \frac{4R_a R_c}{|Z_a + Z_c|^2} \tag{2}$$

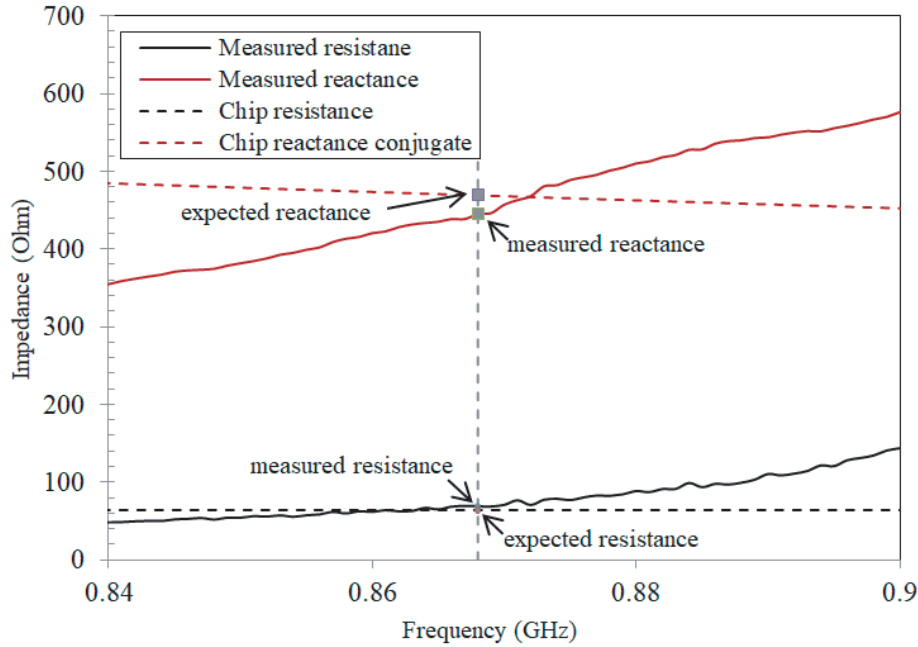


Figure 5. Input impedance of the antenna measured using image theory.

where $Z_a = R_a + jX_a$ is the antenna's input impedance while $Z_c = R_c + jX_c$ is the chip impedance. The proposed antenna has a power transmission coefficient of 0.996 which is very close to the perfectly matching condition.

3.2. Bandwidth

As per the simulation results, the proposed antenna resonates at 868 MHz with $S_{11} = -50.08$ dB having an $S_{11} \leq -10$ dB bandwidth in the range of 690 MHz–970 MHz (Figure 6). Thus, the antenna covers the entire UHF RFID bandwidth defined for any country or region.

3.3. Field Pattern

The measurement setup used to test the field characteristics of the tag inside an anechoic chamber is shown in Figure 7. The measurement was performed using the Nordic ID Sampo, a commercial UHF RFID reader that is compatible with the EPC Class 1 Gen 2 (ISO 18000-6C) standard. The reader features a circularly polarized integrated antenna with a gain of 5 dBi [35].

The tag was placed inside the chamber keeping three different distances ($d = 0.2$ m, 0.3 m, 0.5 m) between the tag and the reader. The reader and the tag were oriented towards the direction of maximum gain, as identified by simulating radiation patterns (Figure 8). At each distance, the reader's output power was varied with a step size of 1 dBm to determine the minimum power (P_{\min}) required to communicate with the tag. The visual indicator of the tag further confirmed the detectability of the tag in each measurement.

As per the results depicted in Figure 9(a), the proposed tag is detectable in the entire UHF band (860 MHz–960 MHz), and a minimum power of 25 dBm was required to establish a communication at 868 MHz frequency, when the distance between the tag and the antenna is 50 cm. The power requirement was lower for shorter distances, and only 13 dBm was required to communicate over a distance of 20 cm. The tag works beyond the corresponding wavelength (35 cm at 868 MHz) as well as very short lengths much lower than the corresponding wavelength, indicating that it effectively performs both the near-field and far-field communication. For further investigation, another set of measurements were taken inside the anechoic chamber, varying the distance between the tag and the reader in the range of 0.2–1 m

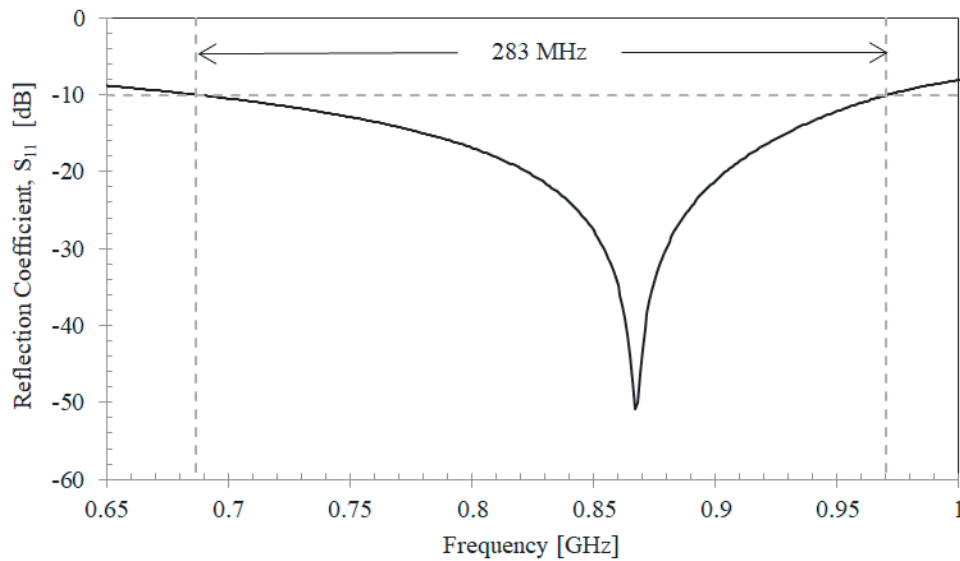


Figure 6. Simulated reflection coefficient.

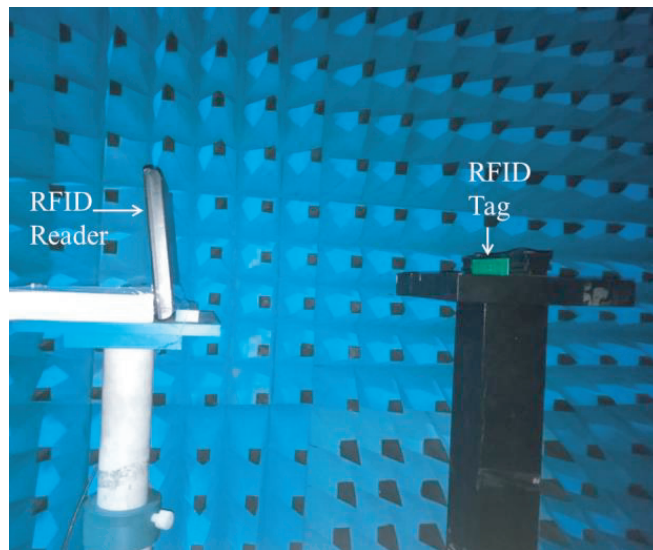


Figure 7. Measurement set up inside an anechoic chamber.

having a step size of 10 cm. The minimum power requirement was plotted as a function of distance at the desired frequency, i.e., 868 MHz (Figure 9(b)).

According to the behavior shown in Figure 9(b), the near-field region at 868 MHz is approximately 40 cm. The proposed tag is detectable up to 1 m distance proving that it performs far-field communication too. The far-field communication is obvious as the UHF dipole facilitates it. In order to investigate the performance of the tag in the near-field region, the surface current distribution and magnetic field distribution of the antenna were simulated at 868 MHz (Figure 10). It can be clearly observed that the surface current and magnetic field are highly concentrated on the T-match loop and gradually decrease towards the folded arms. As per the simulation results, a considerably large current is produced at the loop structure, which results in a strong magnetic field facilitating near-field communication.

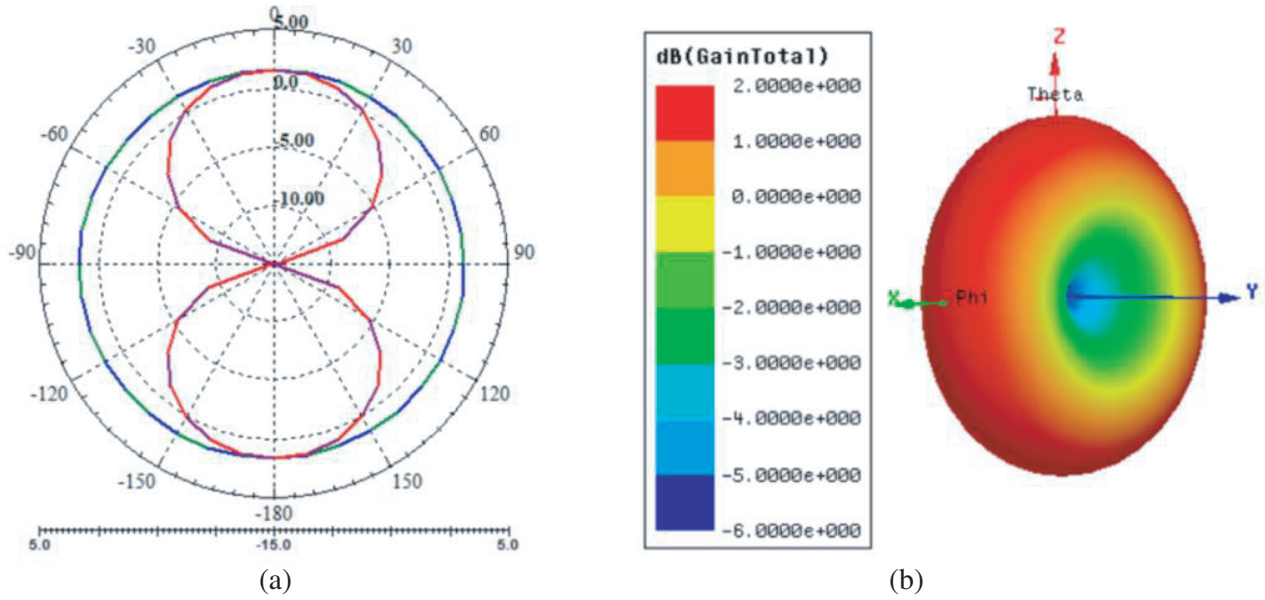


Figure 8. Radiation patterns. (a) Radiation cuts. (b) 3-D pattern.

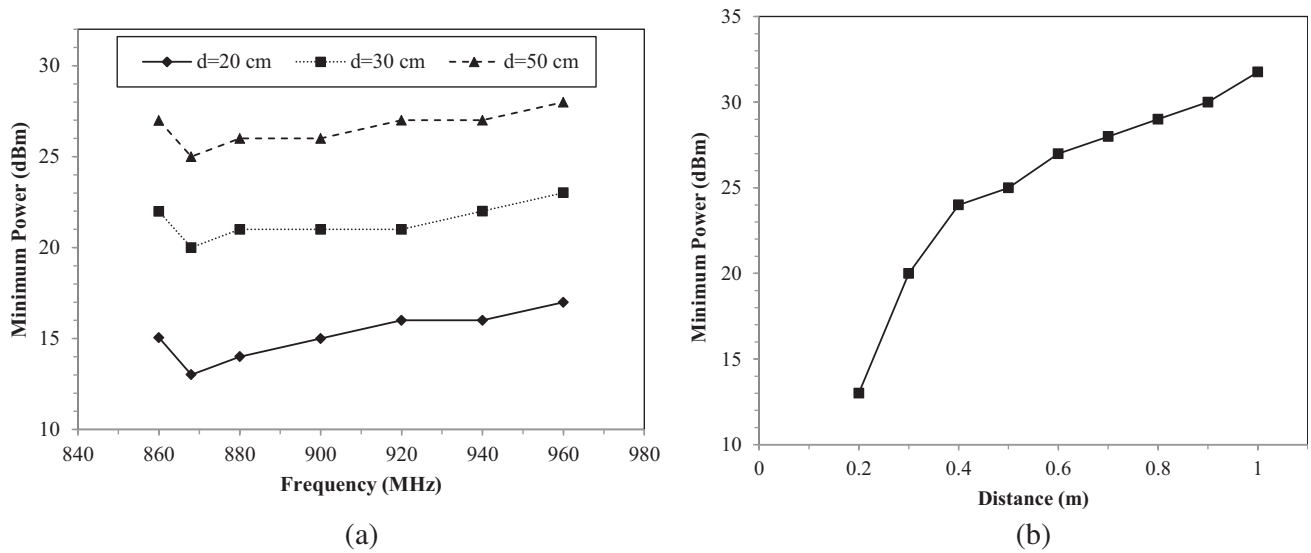


Figure 9. Field measurements. (a) Minimum power vs. frequency. (b) Minimum power vs. distance.

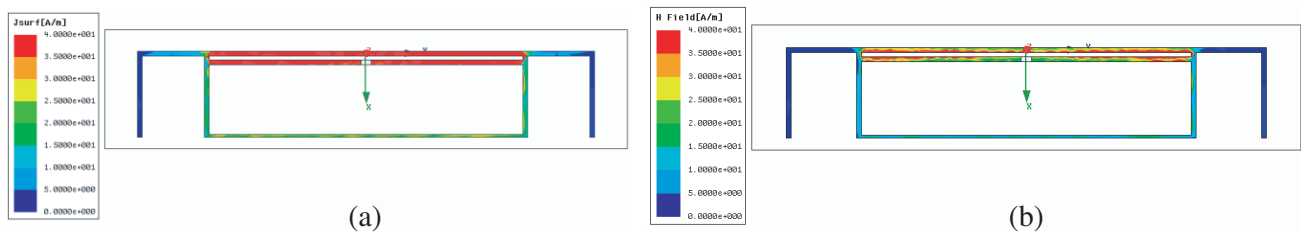


Figure 10. Simulated field patterns at 868 MHz. (a) Surface current distribution. (b) Magnetic field distribution.

4. DISCUSSION AND CONCLUSION

4.1. Discussion

With the growing need for adopting advanced RFID technologies into traffic law enforcement applications, novel and reliable energy harvesting UHF RFID tags with innovative features are essential to overcome the limitations of existing systems. The RFID tag proposed in this paper can be used to effectively read, store, and communicate not only the primary details of the vehicle and the owner, but also legal information such as vehicle registration, smoke certification, and law violation history. Such details are useful for identifying stolen vehicles even when the number plate has been fraudulently changed and to verify the legal compliance. In contrast to existing RFID tags that may be attached to automobiles, the proposed tag can incorporate multiple sensors, is durable, and is compact in size due to the absence of external lumped components for impedance matching.

The tag's detection range is a major concern regarding the use of RFID as it decides the accessibility of stored information. Despite having many advantages, RFID technology has raised a number of concerns in this regard, including the possibility that unauthorized parties could obtain tag information and use it for unlawful acts. A short to medium range (a few tens of centimeters up to one meter) communication is ideal for privacy-related applications. The proposed tag exhibits a constrained detection range while performing well at short distances thanks to the loop configuration coupled with the main dipole. Moreover, as the proposed tag is designed with a visual indicator, the vehicle owner can observe the detection of the tag by a reader.

The size of the tag, durability, and cost ultimately determine the potential of adopting RFID over other similar technologies. These requirements are well met by the proposed tag thanks to its miniaturized configuration and internal impedance matching that eliminates connecting electronic components. Further, the dielectric substrate, FR4, is very cheap and widely available.

Though internal impedance matching mechanisms are becoming more and more popular, they were usually applied only in RFID tags with no sensor integration capability. The chips that enable the integration of sensors to RFID tags have a highly capacitive reactance. Thus, the antennas in chip-based RFID sensor tags need to be highly inductive for impedance matching. For such designs, a scientific approach with technical expertise is required. The performance of chip-based passive UHF RFID sensor tags proposed by researchers, in which different design techniques were applied, is illustrated in Table 1.

As indicated in Table 1, sensor tags made with the SL900A chip utilized an external lumped element matching network. As the resultant antennas reported in [36–38] were lengthy, the dipole arms were bent to reduce the tag size. The arms widths were also kept large to accommodate the sensors, and no other substantial miniaturization methods were applied. The size of the tag designed with the EM4325 chip [39] is comparatively small since its input impedance is lower than that of other RFID sensor chips. However, the chip (EM4325) has less application than the Rocky100 chip since it does not permit the integration of external sensors. In [40], the authors have used the Rocky100 chip in designing a UHF RFID passive sensor tag. An external matching network was used to provide impedance matching

Table 1. Performance of chip-based passive UHF RFID sensor tags.

Reference	Overall size of the tag (mm × mm)	Chip/Input Impedance (Ω)	Design techniques
[36]	107.23 × 38.2	AMS SL900A 123 – j 303	Folded dipole antenna with external impedance matching circuit
[37]	100 × 180		
[38]	Not mentioned		
[39]	35 × 35	EM4325 23.3 – j 145	Loop antenna configuration with internal T-matching
[40]	135 mm in length	Farsens Rocky 100 64 – j 469	Straight dipole antenna with external matching circuit

particularly, incorporating two SMD inductors to compensate the highly capacitive reactance of the chip ($j469\ \Omega$). No any tag designed using the Rocky100 chip reported the use of miniaturization strategies.

Further, a range of battery-free chip-based RFID sensor tags have been developed by Farsens using Rocky100 chips such as STELLA-R [41], HYGRO-FENIX-RM [42], and FENIX-RM [43]. All of them employed a planer dipole antenna with external lumped elements for impedance matching. As no miniaturization techniques were used, the tags are quite lengthy over 130 mm, and the width is around 15 mm. The thicknesses of all the tags are 10 mm. Thus, these tags make a bulky configuration.

Therefore, as compared to the relevant research studies and existing commercial products, the proposed tag is compact, lightweight, and has a longer lifetime. With the internal impedance matching structure, the requirement for external matching components was eliminated, which reduced the tag's material and fabrication costs. As a result, the tags may be produced more cheaply with less complexity.

Moreover, Farsens Rocky100 is the RFID sensor chip with the highest capacitance in the input reactance ($469\ \Omega$). The internal impedance matching of this chip proves that the same research methodology can be applied to any other RFID sensor chips, as their capacitance is not that much high.

There are several research studies on implementing RFID platforms for traffic law enforcement including vehicle registration and data management using off-the-shelf RFID devices [12–14]. The proposed tag thus can be used in such already developed platforms, overcoming the drawbacks of the existing tags.

Although low frequency (LF) and high frequency (HF) RFID systems can also be used for short-range communication, they exhibit several drawbacks. The detection range of the LF tags are limited to 10 cm or so, while HF tags are detectable up to 1 m. However, both of them exhibit a very slow data transferring rate. The LF and HF tags use large coil antennas, while UHF tags use simple dipole-like antennas that are smaller and easier to fabricate. Consequently, the UHF tags are less expensive than LF and HF tags. Hence, UHF tags are more suitable for law enforcement applications in terms of price, size, and data transfer rate.

5. CONCLUSION

This paper presents the design and fabrication of a chip-based, battery-free energy harvesting UHF RFID tag that is specifically useful for traffic law enforcement applications as it is compact, inexpensive, durable, featured with visual indication, sensor-integratable, and has a perfect detection range for inspection and verification of vehicle-related information. The detection range of the tag is critical for ensuring that the tag is not detected anonymously by a third party. The proposed tag is detected in the range of 0.2–1 m demonstrating its suitability for traffic law enforcement by police inspectors. The selected substrate material and the miniaturized tag size were very useful for manufacturing an inexpensive tag. The absence of electronic components achieved by internal impedance matching was helpful to keep a planar configuration. The overall tag size of $110 \times 25 \times 2.4\ \text{mm}^3$ enables attaching it easily on a suitable place of the vehicle. As the chip utilized in the proposed tag supports sensor integration, it has a great potential to widen the applications by adding low power sensors such as temperature sensors, light sensors, and humidity sensors, in contrast to existing RFID tags that can be attached to the vehicles.

ACKNOWLEDGMENT

This work was supported by the Indo-Sri Lanka joint research programme (2019). The authors would like to acknowledge Mr. Tharanga Premathilaka, Senior Electronics Engineer, Techlabs Global PVT Ltd for his assistance with the tag fabrication process.

REFERENCES

1. Parthiban, P., "Embeddable miniature UHF RFID near-field antenna for healthcare applications," *Progress In Electromagnetics Research M*, Vol. 87, 199–207, 2019.

2. Raihani, H., A. Benbassou, M. El Ghzaoui, and J. Belkaid, "Performance evaluation of a passive UHF RFID tag antenna using the embedded T-match structure," May 2017, doi: 10.1109/WITS.2017.7934636.
3. Prahlad, N. S., P. A. N. Venkat, and M. R. Ahmed, "Design of an U shaped slotted patch antenna for RFID vehicle identification," *Proceedings of the 2nd International Conference on Green Computing and Internet of Things, ICGCIoT 2018*, 300–304, Aug. 2018.
4. García Oya, J. R., R. Martín Clemente, E. Hidalgo Fort, R. González Carvajal, and F. Muñoz Chavero, "Passive RFID-based inventory of traffic signs on roads and urban environments," *Sensors 2018*, Vol. 18, No. 7, 2385, Jul. 2018.
5. Chowdary Polavarapu, S., U. Kunduru, and H. Nallamala, "RFID based automatic tollgate collection," *Int. J. Eng. Technol.*, Vol. 7, No. 2, 1–5, 2018.
6. Van Hoang, T. Q., D. H. N. Bui, T. P. Nguyen, T. P. Vuong, and C. Defay, "Passive battery-free UHF RFID tag for athermic car windshields," *2017 IEEE Antennas and Propagation Society International Symposium, Proceedings*, Vol. 2017-January, 643–644, Oct. 2017.
7. Agarwal, V., S. Sharma, and P. Agarwal, "IOT based smart transport management and vehicle-to-vehicle communication system," *Comput. Networks, Big Data IoT 2021*, Vol. 66, 709–716, 2021.
8. Gowri, S., J. S. Vimali, D. U. Karthik, and G. A. John Jeffrey, "Real time traffic signal and speed violation control system of vehicles using IOT," *Lect. Notes Data Eng. Commun. Technol.*, Vol. 49, 953–958, 2020.
9. Atta, A., S. Abbas, M. A. Khan, G. Ahmed, and U. Farooq, "An adaptive approach: Smart traffic congestion control system," *J. King Saud Univ. — Comput. Inf. Sci.*, Vol. 32, No. 9, 1012–1019, Nov. 2020.
10. Al-abassi, S. A. W., K. Y. A. Al-bayati, M. R. R. Sharba, and L. Abogneem, "Smart prepaid traffic fines system using RFID, IoT and mobile app," *TELKOMNIKA (Telecommunication Comput. Electron. Control)*, Vol. 17, No. 4, 1828–1837, Aug. 2019.
11. Naik, T., R. Roopalakshmi, N. Divya Ravi, P. Jain, B. H. Sowmya, and Manichandra, "RFID-based smart traffic control framework for emergency vehicles," *Proc. Int. Conf. Inven. Commun. Comput. Technol., ICICCT 2018*, 398–401, Sep. 2018.
12. Vishnevsky, V. M., A. Larionov, and R. Ivanov, "Architecture of application platform for RFID-enabled traffic law enforcement system," *2014 7th International Workshop on Communication Technologies for Vehicles, Nets4Cars-Fall 2014*, 45–49, Dec. 2014.
13. Hoffman, A. J. and A. J. Pretorius, "SmartRoad: A New Approach to Law Enforcement in Dense Traffic Environments," *IEEE Conf. Intell. Transp. Syst. Proceedings, ITSC*, Vol. 2015-October, 598–605, Oct. 2015.
14. Vishnevsky, V. M. and A. Larionov, "Design concepts of an application platform for traffic law enforcement and vehicles registration comprising RFID technology," *2012 IEEE International Conference on RFID-Technologies and Applications, RFID-TA 2012*, 148–153, 2012.
15. Grosinger, J., W. Pachler, and W. Bosch, "Tag size matters: Miniaturized RFID tags to connect smart objects to the internet," *IEEE Microw. Mag.*, Vol. 19, No. 6, 101–111, Sep. 2018.
16. Chung, Y. and T. H. Berhe, "Long-range UHF RFID tag for automotive license plate," *Sensors 2021*, Vol. 21, No. 7, 2521, Apr. 2021.
17. "Impinj Monza 4 RAIN RFID Tag Chips — IMPINJ," <https://www.impinj.com/products/tag-chips/impinj-monza-4-series> (accessed May 01, 2023).
18. "IC-Alien Technology," <https://www.alientechnology.com/products/ic/> (accessed May 01, 2023).
19. Nguyen, V. H., A. Diallo, P. Le Thuc, R. Staraj, S. Lanteri, and G. F. Carle, "A miniature implanted antenna for UHF RFID applications," *Progress In Electromagnetics Research C*, Vol. 99, 221–238, 2020.
20. Shaikh, K. M., K. J. Karande, and S. V. Surwase, "Nested slot suspended patch antenna using CST microwave studio," Nov. 2018, doi: 10.1109/ICICET.2018.8533805.

21. Choudhary, A., K. Gopal, D. Sood, and C. C. Tripathi, "Development of compact inductive coupled meander line RFID tag for near-field applications," *Int. J. Microw. Wirel. Technol.*, Vol. 9, No. 4, 757–764, May 2017.
22. "RFID inlay/label/tag factory/Farsens Rocky100," <https://www.richrfid.com/epc-c1g2-batteryless-pressure-sensor.html> (accessed June 23, 2023).
23. Kumar, M., A. Sharma, and I. J. G. Zuazola, "All-in-One UHF RFID tag antenna for retail garments using nonuniform meandered lines," *Progress In Electromagnetics Research Letters*, Vol. 94, 133–139, 2020.
24. Jalal, A. S. A. and A. Ismail, "A compact fractal-based asymmetrical dipole antenna for RFID tag applications," *2018 3rd Scientific Conference of Electrical Engineering, SCEE 2018*, 101–104, Jul. 2018.
25. Moh, C. W., E. H. Lim, F. L. Bong, and B. K. Chung, "Miniature coplanar-fed folded patch for metal mountable UHF RFID tag," *IEEE Trans. Antennas Propag.*, Vol. 66, No. 5, 2245–2253, May 2018.
26. Michel, A., P. Nepa, X. Qing, and Z. N. Chen, "Considering high-performance near-field reader antennas: Comparisons of proposed antenna layouts for ultrahigh-frequency near-field radio-frequency identification," *IEEE Antennas Propag. Mag.*, Vol. 60, No. 1, 14–26, Feb. 2018.
27. Sundaram, B. R., S. K. Vasudevan, E. Aravind, G. Karthick, and S. Harithaa, "Smart car design using RFID," *Indian J. Sci. Technol.*, Vol. 8, No. 11, 1–5, 2015.
28. Dhaouadi, M., M. Mabrouk, T. P. Vuong, A. C. De Souza, and A. Ghazel, "UHF tag antenna for near-field and far-field RFID applications," *WAMICON 2014*, 2014.
29. Yao, Y., Y. Liang, J. Yu, and X. Chen, "Design of a multipolarized RFID reader antenna for UHF near-field applications," *IEEE Trans. Antennas Propag.*, Vol. 65, No. 7, 3344–3351, Jul. 2017.
30. Michel, A., A. Buffi, R. Caso, P. Nepa, G. Isola, and H. T. Chou, "Design and performance analysis of a planar antenna for near-field UHF-RFID desktop readers," *Asia-Pacific Microwave Conference Proceedings, APMC*, 1019–1021, 2012.
31. Dhaouadi, M., M. Mabrouk, A. Ghazel, and S. Tedjini, "Electromagnetic analysis of UHF near-field RFID tag antenna," 2011, doi: 10.1109/URSIGASS.2011.6050654.
32. Ennasar, M. A., O. El Mrabet, K. Mohamed, and M. Essaaidi, "Design and characterization of a broadband flexible polyimide RFID tag sensor for NaCl and sugar detection," *Progress In Electromagnetics Research C*, Vol. 94, 273–283, 2019.
33. Wickramasinghe, S., J. Jayasinghe, and M. Senadeera, "Design of a passive RFID tag antenna with a modified T-match structure," *2021 IEEE 16th Int. Conf. Ind. Inf. Syst. ICIIS 2021 — Proc.*, 46–51, 2021.
34. Aznabet, I., M. A. Ennasar, O. El Mrabet, G. Andia Vera, M. Khalladi, and S. Tedjini, "A broadband modified T-shaped planar dipole antenna for UHF RFID tag applications," *Progress In Electromagnetics Research C*, Vol. 73, 137–144, 2017.
35. "Nordic ID Sampo S1 datasheet v18 — Nordic ID," <https://www.nordicid.com/nordic-id-sampo-s1-datasheet-v18/> (accessed Oct. 03, 2022).
36. Abdelnour, A., N. Fonseca, A. Rennane, D. Kaddour, and S. Tedjini, "Design of RFID sensor tag for cheese quality monitoring," *IEEE MTT-S International Microwave Symposium Digest*, Vol. 2019-June, 290–292, Jun. 2019.
37. Pichorim, S. F., N. J. Gomes, and J. C. Batchelor, "Two solutions of soil moisture sensing with RFID for landslide monitoring," *Sensors 2018*, Vol. 18, No. 2, 452, Feb. 2018.
38. Rennane, A., N. Fonseca, A. Abdelnour, et al., "Passive UHF RFID sensor tag for pressure and temperature conditions monitoring," Sep. 2018, doi: 10.23919/URSI-AT-RASC.2018.8471459.
39. Occhiuzzi, C., S. Parrella, F. Camera, S. Nappi, and G. Marrocco, "RFID-based dual-chip epidermal sensing platform for human skin monitoring," *IEEE Sens. J.*, Vol. 21, No. 4, 5359–5367, Feb. 2021.

40. Vena, A., B. Sorli, B. Saggin, R. Garcia, and J. Podlecki, "Passive UHF RFID sensor to monitor fragile objects during transportation," *2019 IEEE International Conference on RFID Technology and Applications, RFID-TA 2019*, 415–420, Sep. 2019.
41. "RFID inlay/label/tag factory/STELLA-R," <https://www.richrfid.com/epc-c1g2-batteryless-led-indicator.html> (accessed June 23, 2023).
42. "RFID inlay/label/tag factory/HYGRO-FENIX-RM," <https://www.richrfid.com/epc-c1g2-batteryless-ambient-temperature-and-relative-humidity-sensor-2.html> (accessed June 23, 2023).
43. "RFID inlay/label/tag factory/FENIX-RM," <https://www.richrfid.com/epc-c1g2-batteryless-ambient-temperature-sensor-2.html> (accessed June 23, 2023).